Net heat current at zero mean temperature gradient

Jose Ordonez-Miranda, Roman Anufriev, Masahiro Nomura, Sebastian Volz

Letter

Net heat current at zero mean temperature gradient

Jose Ordonez-Miranda [1,2,*] Roman Anufriev [2] Masahiro Nomura [2,1] and Sebastian Volz [1,2]
[1]*LIMMS, CNRS-IIS UMI 2820, The University of Tokyo, Tokyo 153-8505, Japan*
[2]*Institute of Industrial Science, The University of Tokyo, Tokyo 153-8505, Japan*

(Received 25 June 2022; revised 30 August 2022; accepted 1 September 2022; published 9 September 2022)

The existence of a net heat current of conductive thermal waves is demonstrated even in the absence of a mean temperature gradient. This effect, which we called heat shuttling, is generated by the temperature-dependent thermal conductivity of materials excited with a thermal excitation periodically modulated in time. We show that this modulation gives rise to a heat current superimposed on the one generated by the mean temperature gradient, which enhances the heat transport when the thermal conductivity increases with temperature. By contrast, if the thermal conductivity decreases as temperature increases, the thermal-wave heat current inverts its direction and reduces the total heat flux. The reported shutting effect is sensitive to the amplitude of the periodic thermal excitation, which can facilitate its observation and application to harvest energy from the temperature variations of the environment.

DOI: 10.1103/PhysRevB.106.L100102

Nonlinear heat conduction determined by a temperature dependent thermal conductivity is of primary importance to tailor heat currents driving a wide variety of technologies [1–3]. This thermal dependence generates an asymmetric material response that has been used to develop thermal analogs of electronic devices, including thermal diodes [4–9], thermal transistors [10,11], thermal logic gates [12], thermal memories [13], and thermal memristors [14,15]. Based on the asymmetric transitions of two phase change materials (PCMs) with thermal conductivities strongly varying in a narrow interval of temperatures, Shen *et al.* [16] developed a temperature-trapping theory and proposed an energy-free thermostat able to self-maintain a desired constant temperature without consuming energy, regardless of the sizable changes of its environmental temperature. More recently, Wang *et al.* [17] introduced thermoelectric effects in this latter theory and proposed a negative-energy thermostat capable of generating electricity with energy-free maintenance of a constant ambient temperature.

Thermal modulation naturally occurs in many systems due to the temperature fluctuations of the environment. However, until now, very few works studied the nonlinear heat transport under dynamical conditions [18–20]. By exciting a nonlinear asymmetric lattice with a temperature difference periodically modulated in time, the appearance of a net heat current was predicted in absence of an average thermal bias [21–23]. More recently, by imposing a sinusoidal temperature excitation on two counter-moving media, Li *et al.* [1] demonstrated the antiparity-time symmetry in diffusive systems. This type of thermal sources has also been applied to generate exotic effects, such as the reciprocity of thermal diffusion [24], the configurable phase transitions of a topological material [25], and the rectification of thermal-wave heat currents [26]. This fine tuning of dynamical heat fluxes in idealized microscopic nonlinear lattices and moving systems is also expected to be possible with PCMs, whose thermal properties depend strongly on temperature. In particular, the periodic thermal excitation of PCMs could lead to net heat fluxes driven by conductive thermal waves, which usually carry a zero mean heat flux, in materials with constant thermal properties [27]. Even though these waves are widely applied to determine thermal properties via standard techniques, such as thermoreflectance [28], photothermal radiometry [29], 3ω [30], photoacoustics [13], and resonant cavity [6]; their contribution to the total heat flux in PCMs has not been explored yet.

In this Letter, we theoretically demonstrate the existence of the conductive heat shuttling, a net heat current generated by thermal waves that shows up even in the absence of a mean temperature gradient. This shuttling effect paves the way to manage conductive heat currents in nonlinear systems out of equilibrium.

Let us consider two thermal baths exchanging heat through conduction in a PCM of length l, due to their temperature difference $T_h - T_c + \delta T(t)$ periodically modulated in time t, as shown in Fig. 1. The thermal conductivity $k(T)$ and volumetric heat capacity $C(T)$ of the PCM depends on its temperature T, as is the case of VO_2, nitinol [7,31], and any material in a large enough interval of temperatures. Considering that the surfaces $x = 0$ and l are uniformly heated up by the thermal baths, the one-dimensional heat conduction in the material is characterized by the spatiotemporal distribution of its temperature $T(x,t)$ and heat flux $q(x,t)$ given respectively by the diffusion equation and Fourier's law, as follows:

$$\frac{\partial}{\partial x}\left(k(T)\frac{\partial T}{\partial x}\right) = C(T)\frac{\partial T}{\partial t}, \tag{1a}$$

$$q = -k(T)\frac{\partial T}{\partial x}. \tag{1b}$$

*jose.ordonez@cnrs.fr

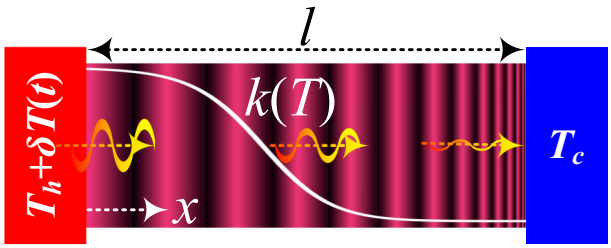

FIG. 1. Scheme of a PCM supporting the heat conduction between two thermal baths due to their temperature difference $T_h - T_c + \delta T(t)$. Arrows and their amplitudes indicate the propagation direction and intensity of the thermal waves generated by the periodic excitation $\delta T(t) = \Delta T S(t)$ with $0 < \Delta T \ll T_h$ and $|S(t)| \leqslant 1$. The white line stands for the VO_2 thermal conductivity varying from a high value, near the left hot bath, to a low one close to the right cold bath.

The temperature satisfies the boundary conditions $T(0,t) = T_h + \delta T(t)$ and $T(l,t) = T_c$, with $\delta T(t)$ being a periodic function of time with values much smaller than its steady-state counterpart ($|\delta T(t)| \ll T_h$). For this external excitation, the solution of Eq. 1(a) for the temperature T has the following general solution

$$T(x,t) = \psi(x) + \theta(x,t), \tag{2}$$

where $\theta = a_0/2 + \sum_{n=1}^{\infty}[a_n \cos(2\pi nt/\tau) + b_n \sin(2\pi nt/\tau)]$ is a periodic function with period τ and module $|\theta| \ll \psi$. The parameters $a_0(x)$, $a_n(x)$, and $b_n(x)$ are the usual Fourier's coefficients defined for an arbitrary periodic function. As the steady-state temperature component is defined by ψ in Eq. (2), we take $a_0 = 0$. Because of the relatively small values of θ with respect to ψ, the PCM thermal conductivity can be expanded in power series of θ by means of the Taylor's series expansion $k(T) = k(\psi) + \theta k'(\psi) + ...$, which in combination with Eq. 1(b) yields:

$$q = -k\frac{\partial(\psi+\theta)}{\partial x} - k'\left(\theta\frac{d\psi}{dx} + \frac{1}{2}\frac{\partial\theta^2}{\partial x}\right) - \frac{k''}{2}\frac{d\psi}{dx}\theta^2, \tag{3}$$

where $k = k(\psi)$, $k'(\psi) = dk(\psi)/d\psi$, $k''(\psi) = d^2k(\psi)/d\psi^2$, and an approximation up to θ^2 was considered. The average heat flux $\bar{q}(x) = \tau^{-1}\int_0^\tau q(x,t)dt$ over one period τ is then given by

$$\bar{q}(x) = -k(\psi)\frac{d\psi}{dx} - \frac{k'(\psi)}{2}\frac{d\bar{\theta^2}}{dx} - \frac{k''(\psi)}{2}\frac{d\psi}{dx}\bar{\theta^2}, \tag{4}$$

where $\bar{\theta}(x) = a_0(x)/2 = 0$ was used and

$$\bar{\theta^2} = \frac{1}{\tau}\int_0^\tau \theta^2(x,t)dt = \frac{1}{2}\sum_{n=1}^{\infty}\left(a_n^2(x) + b_n^2(x)\right). \tag{5}$$

For a temperature-independent thermal conductivity ($k =$ constant), the net heat flux in Eq. (4) reduces to its steady-state counterpart ($q_{ss} = -k(\psi)d\psi/dx$), as expected. By contrast, if k does depend on temperature, the periodic excitation $\delta T(t)$ generates the following net contribution to the heat flux:

$$\bar{q}(x) - q_{ss} = -\frac{1}{4}\frac{d}{dx}\left[k'(\psi)\sum_{n=1}^{\infty}\left(a_n^2(x) + b_n^2(x)\right)\right]. \tag{6}$$

The propagation of thermal waves in a PCM therefore generates a net heat flux driven by the slope of the temperature dependent thermal conductivity. According to Eq. (6), this heat current is present even in absence of a net temperature gradient ($T_h = T_c = \psi$), provided that the average value of the periodic excitation vanishes ($\delta\bar{T}(t) = \Delta T\bar{S}(t) = 0$), as considered in Eq. (4) for $x = 0$. This latter condition is well satisfied by the harmonic function $S(t) = \cos(\omega t)$ that is commonly used for the generation of thermal waves. For $T_h = T_c = \psi$, $q_{ss} = 0$ and $\bar{q} \propto k'(\psi)$, which provides an effective way to control the direction of the heat flux shuttling. If the thermal conductivity increases with temperature ($k'(\psi) > 0$), the thermal-wave heat flux propagates from the thermal bath with a modulated temperature to the one with a steady-state temperature, reversing its direction for $k'(\psi) < 0$. As the thermal conductivity of most materials depends on temperature and the net heat flux of thermal waves is proportional to the slope of thermal conductivity [see Eq. (6)], this heat shuttling is generally expected to appear in almost any solid material and is analogous to the enhanced thermal convection observed in fluids subjected to temperature gradients periodically modulated in time [32,33].

The effect of thermal energy harvesting in a dynamical system without a mean temperature gradient will now be quantified for VO_2, a PCM with a sharp metal-insulator transition (MIT) spanning from about 340 to 345 K. The thermal conductivity of VO_2 varies between its values at the insulating ($k_i = 3.6$ $Wm^{-1}K^{-1}$) and metallic ($k_m = 6$ $Wm^{-1}K^{-1}$) phases, and its temperature evolution is well described by [7]

$$k(T) = k_i + \frac{k_m - k_i}{1 + \exp\left[-\beta(T - T_0)\right]}, \tag{7}$$

where $\beta = 1.6$ K^{-1} and $T_0 = 342.9$ K is the VO_2 transition temperature. As k in Eq. (7) increases with T, when the oscillations of the thermal excitation swing up ($S > 0$), the thermal conductivity is higher than when they swing down ($S < 0$). This thermal conductivity difference provides more facility to the thermal waves for traveling forward than backward, which generates a nonzero heat flux. The volumetric heat capacity of VO_2, on the other hand, is given by [34] $C = \rho(c_D(T) + Ldf(T)/dT)$, with $\rho = 4612$ kg m^{-3} and $L = 50.75$ kJ kg^{-1} being its respective density and latent heat, $c_D(T)$ is the Debye specific heat capacity with $T(\text{Debye}) = 750$ K, and $f(T)$ is the volume fraction of the metallic domains of VO_2 during its MIT [34]. As $k'(\psi)$ is greater than zero and reaches its peak at $\psi = T_0$, Eq. (6) indicates that the shuttling heat flux propagates from left to right (see Fig. 1) and takes its maximum value at the VO_2 transition temperature. Lower and higher temperatures weakens the shuttling effect until disappearing it outside the MIT of VO_2 ($k'(\psi) \to 0$), as shown below. Equation 1(a) does not have an analytical general solution for these thermal properties $k(T)$ and $C(T)$ plotted in the Supplemental Material (SM) [35], and therefore its solution will numerically be obtained by using the finite element method (FEM) via the software Comsol multiphysics. However, if the modulation frequency ω of the thermal excitation $\delta T(t) = \Delta T\cos(\omega t)$ is low enough and/or the length l is sufficiently small, the transient effects can be neglected ($\partial T/\partial t \to 0$) and Eq. 1(a) becomes independent of the heat capacity. For a material with

constant thermal properties, this quasisteady state regime is reached for $\omega \ll 2k/Cl^2$ (thermally thin material), as shown in the SM [35]. Under this thermally-thin condition, the analytical integration of Eq. 1(a) yields

$$T - T_0 + \frac{1}{\beta\lambda}\ln[1 + Z(T)] = C - \frac{q}{k_m}x, \tag{8}$$

where C is an integration constant, $\lambda = k_m/(k_m - k_i)$, and $Z(T) = \exp[-\beta(T - T_0)]$. The evaluation of Eq. (8) at the PCM surfaces $x = 0; l$ (see Fig. 1) determines both q and C, which allows expressing the heat flux and temperature distribution as follows

$$q = \frac{k_m - k_i}{\beta l}\ln\left[\frac{f(T_h + \Delta T\cos(\omega t))}{f(T_c)}\right], \tag{9a}$$

$$f(T) = [f(T_h + \Delta T\cos(\omega t))]^{1-x/l}[f(T_c)]^{x/l}, \tag{9b}$$

where $f(\xi) = [1 + Z(\xi)][Z(\xi)]^{-\lambda}$. As a result of the VO_2 MIT ($k_m \neq k_i$), q and T exhibit a nonlinear dependence on the periodic thermal excitation. This strong nonlinearity also holds for the spatial distribution of the temperature profile. According to Eq. 9(a), the thermal-wave heat flux $q(T_h, T_h, \Delta T) = q(T_h, T_c, \Delta T) - q(T_h, T_c, 0)$ is independent of T_c and is driven by the steady-state temperature component T_h of the oscillating excitation. For temperatures out of the MIT, Eq. 9(a) reduces to $q = k_i[T_h - T_c + \Delta T\cos(\omega t)]/l$ for $T_h + \Delta T$; $T_c \ll T_0$, and $q = k_m[T_h - T_c + \Delta T\cos(\omega t)]/l$ for $T_h - \Delta T$; $T_c \gg T_0$, as expected. For both limiting cases, the temperature recovers its usual linear spatial profile $T = (T_h + \Delta T\cos(\omega t))(1 - x/l) + T_c x/l$ that appears for thermal waves propagating in thermally thin materials with constant properties [35]. In these cases, the linear dependence of q and T on the modulated excitation $\Delta T\cos(\omega t)$ cancels out its contribution to their average values $\bar{q}$ and $\bar{T}$ over one period $\tau = 2\pi/\omega$. It is thus clear that at least one of the temperatures T_h and T_c should be within the MIT to generate the heat flux shuttling driven by ΔT. For a given T_c, one can show that the maximum of $\bar{q}$ in Eq. 9(a) shows up at $T_h = T_0$ that maximizes $k'(T_h)$. In this case, the uppermost heat flux shuttling is given by [35]

$$\bar{q} - q_{ss} = \frac{(k_m - k_i)\Delta T}{\pi l}\left[1 - \pi\frac{\ln(2) - S(\beta\Delta T)}{\beta\Delta T}\right], \tag{10a}$$

$$S(\xi) = \sum_{n=0}^{\infty}\frac{(-1)^n}{n+1}\{I_0[(n+1)\xi] - L_0[(n+1)\xi]\}, \tag{10b}$$

where $q_{ss} = \bar{q}|_{\Delta T=0}$, and I_0 and L_0 are the modified Bessel and Struve functions, respectively. The heat flux difference $\bar{q} - q_{ss}$ thus represents the maximum contribution of the thermal waves generated by the periodic excitation with amplitude ΔT. In consistence with Eq. (6), this heat shuttling is strongly driven by $k'(T_0) = (k_m - k_i)\beta/4$ and shows up even in the absence of a net temperature gradient ($T_h = T_c$). The function $S(\beta\Delta T) < \ln(2)$ monotonically decreases as $\beta\Delta T$ increases and therefore the heat shuttling strengthens for higher amplitudes ΔT and/or steeper MIT (larger β), such that $\bar{q} - q_{ss} = (k_m - k_i)\Delta T/\pi l$ for $\beta\Delta T \gg 1$. Furthermore, by taking the spatial derivative of $\ln(f(T))$ determined by Eq. 9(b), one can show that the mean heat flux $\bar{q}$ is related to the average temperature $\bar{T}$ by $\bar{q} = -k(T_2)\partial\bar{T}/\partial x|_{x=l}$. This simple relation

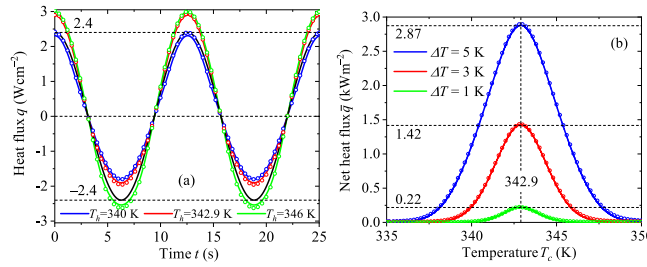

FIG. 2. (a) Time evolution of the heat flux and (b) its average (net) counterpart as a function of the temperature $T_h = T_c$, for three amplitudes of the periodic excitation. The black line in (a) stands for the heat flux in a material with constant thermal conductivity $(k_m + k_i)/2$ and the dots represent the numerical results obtained with FEM. Calculations were done for a VO_2 layer with $l = 1$ mm, $\omega = 0.5$ rad/s, and $\Delta T = 5$ K in (a).

indicates that the shuttling effect in a PCM can be described like the steady-state heat conduction in a non-PCM with constant and effective thermal conductivity $k(T_2)$.

The heat flux oscillations of thermal waves propagating in VO_2 are shown in Fig. 2(a), for three representative temperatures $T_h = T_c$ around its transition temperature. For reference, the black line stands for the heat flux in a non-PCM with constant thermal conductivity $(k_m + k_i)/2$. For this latter material, q is independent of T_h and oscillates around zero with an amplitude of 2.4 W cm^{-2}. By contrast, q in VO_2 oscillates around a positive value with an amplitude that increases with T_h. These heat flux oscillations predicted by Eq. 9(a) are well confirmed by the numerical solution of Eq. 1(a) [dots in Fig. 2(a)] and indicates the presence of a net heat flux $\bar{q}$ propagating from the left thermal bath to the right one, even though they share the same average temperature $T_h = T_c$, as shown in Fig. 2(b). Note that $\bar{q}$ increases with ΔT and takes its highest values at the VO_2 transition temperature $T_h = T_0$ at which $k'(T)$ is maximum, as established by Eq. (6). The highest heat flux transported by thermal waves is well described by Eq. 10(a), whose predictions are shown by the horizontal dashed lines in Fig. 2(b). A higher or lower temperature T_h yields smaller $\bar{q}$ values, which confirms the essential temperature dependence of the thermal conductivity to generate the heat shuttling by thermal waves.

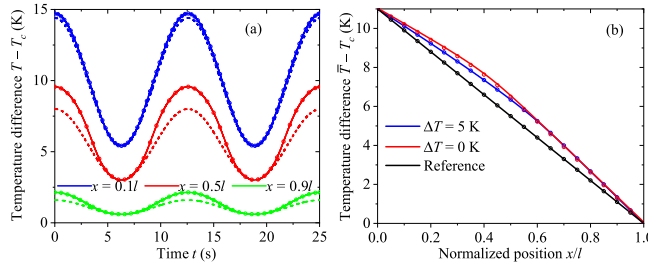

FIG. 3. (a) Time evolution of the temperature difference $\bar{T} - T_c$ and (b) its averaged counterpart as a function of position. The reference black line in (b) stands for the temperature [dashed lines in (a)] in a material with constant thermal conductivity $(k_m + k_i)/2$. Dots represent the FEM calculations done for $(T_h; T_c) = (346; 335)$K, $l = 1$ mm, $\omega = 0.5$ rad/s, and $\Delta T = 5$ K in (a).

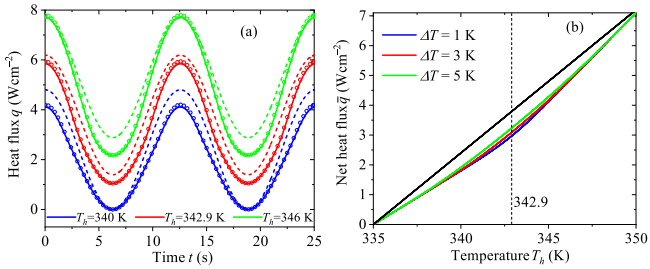

FIG. 4. (a) Time evolution of the heat flux and (b) its averaged counterpart as a function of the temperature $T_h > T_c = 335$ K for three amplitudes of the periodic excitation. The dashed lines in (a) stand for the heat flux in a material with constant thermal conductivity $(k_m + k_i)/2$, whose average value is given by the black line in (b). Dots represent the FEM calculations done for $l = 1$ mm, $\omega = 0.5$ rad/s and $\Delta T = 5$ K in (a).

Figures 3(a) and 3(b) show the respective time variations of the temperature difference $T - T_c$ and the spatial distribution of its averaged counterpart, for $T_h = 346$ K and $T_c = 335$ K spanning over the VO_2 MIT. Note that the amplitude of the temperature oscillations reduces as they travel away from the left thermal bath that generates them, as expected. The analytical predictions of Eq. 9(b) exhibit an accurate agreement with their corresponding numerical ones (dots) and show that temperature in VO_2 is generally higher than that (dashed lines) in a non-PCM with constant thermal conductivity $(k_m + k_i)/2$. This temperature increase tends to vanish at positions ($x = 0.1l$ and $0.9l$) near the thermal baths as a result of their temperatures outside of the MIT. For intermediate positions, on the other hand, the temperature difference tends to increase, which yields an average temperature $\bar{T}$ (blue line) that is nonlinear and higher than the linear one (black line) obtained with a non-PCM, as shown in Fig. 3(b). This deviation from the linear profile represents the fingerprint of the temperature dependent thermal conductivity and is not so different that the corresponding one retrieved under steady-state conditions ($\Delta T = 0$). The propagation of thermal waves in a PCM therefore has a limited impact on its average temperature profile, as assumed in Eq. (3) ($\theta \ll \psi$).

The heat flux and its time average over one period are shown in Figs. 4(a) and 4(b), as functions of time and temperature $T_h > T_c = 335$ K, respectively. In contrast to the heat flux obtained for $T_h = T_c$ [see Fig. 2(a)], q now oscillates through positive values only that are generally smaller than the corresponding ones determined for a non-PCM with constant thermal conductivity. These q values increase with T_h are well confirmed by the numerical FEM simulations (dots), and yield an average heat flux $\bar{q}$ increasing with the modulated temperature amplitude ΔT. The deviation from the linear profile of $\bar{q}$ obtained for a non-PCM (black line) reaches its maximum at the temperature $T_h = T_0$ maximizing $k'(T_h)$, as expected. This nonlinear behavior is driven by the steady-state component $q_{ss} = \bar{q}|_{\Delta T=0}$ of $\bar{q}$, as it reduces for higher amplitudes ΔT driving the propagation of thermal waves. The net contribution $\bar{q} - q_{ss}$ of these waves increases with ΔT and is exactly given by the heat flux shown in Fig. 2(b) for $T_h = T_c$. The heat shuttling is thus independent of T_c, as established by Eq. 9(a), and could be observed for a high enough $\Delta T \geqslant 1$ K.

Even though the thermal-wave heat flux reported in this Letter has been obtained with a single modulation frequency, we anticipate that this shuttling effect can also be achieved with thermal baths set at temperatures oscillating with equal or different frequencies and amplitudes. These parameters represent effective degrees of freedom to tailor the thermal-wave heat flux, as the heat conduction in a PCM is nonlinear and therefore the superposition principle does not apply. Considering the wide applications of thermal waves for detecting thermal phenomena, this customization of the heat shuttling is expected to open new possibilities to tailor and apply not only the temperature field of thermal waves [6,13,28–30], but also their heat flux profile.

In summary, we have demonstrated the existence of a net heat flux driven by thermal waves propagating along a material excited with a temperature difference modulated in time. This heat shuttling is caused by the temperature dependence of the thermal conductivity, its magnitude increases with the slope of the thermal conductivity, and exists even in the absence of an average temperature gradient. In the presence of a net temperature difference, the heat shuttling enables to amplify or reduce steady-state heat currents when the sign of the thermal conductivity slope is positive or negative, respectively. The high sensitivity of the reported shuttling effect to the amplitude of the periodic thermal excitation is expected to facilitate its observation and application to harvest energy from external temperature variations.

[1] Y. Li, Y.-G. Peng, L. Han, M.-A. Miri, W. Li, M. Xiao, X.-F. Zhu, J. Zhao, A. Alú, S. Fan, and C.-W. Qiu, Anti-parity-time symmetry in diffusive systems, Science **364**, 170 (2019).

[2] C. W. Chang, D. Okawa, A. Majumdar, and A. Zettl, Solid-state thermal rectifier, Science **314**, 1121 (2006).

[3] J. Ordonez-Miranda, Radiative Thermostat Driven by the Combined Dynamics of Electrons, Phonons, and Photons, Phys. Rev. Applied **14**, 064043 (2020).

[4] B. Li, L. Wang, and G. Casati, Thermal Diode: Rectification of Heat Flux, Phys. Rev. Lett. **93**, 184301 (2004).

[5] M. Terraneo, M. Peyrard, and G. Casati, Controlling the Energy Flow in Nonlinear Lattices: A Model for a Thermal Rectifier, Phys. Rev. Lett. **88**, 094302 (2002).

[6] J. Hu, X. Ruan, and Y. P. Chen, Thermal conductivity and thermal rectification in graphene nanoribbons: A molecular dynamics study, Nano Lett. **9**, 2730 (2009).

[7] J. Ordonez-Miranda, J. M. Hill, K. Joulain, Y. Ezzahri, and J. Drevillon, Conductive thermal diode based on the thermal hysteresis of VO_2 and nitinol, J. Appl. Phys. **123**, 085102 (2018).

[8] M. Schmotz, J. Maier, E. Scheer, and P. Leiderer, A thermal diode using phonon rectification, New J. Phys. **13**, 113027 (2011).

[9] A. Fornieri, M. J. Martinez-Perez, and F. Giazotto, A normal metal tunnel-junction heat diode, Appl. Phys. Lett. **104**, 183108 (2014).

[10] B. Li, L. Wang, and G. Casati, Negative differential thermal resistance and thermal transistor, Appl. Phys. Lett. **88**, 143501 (2006).

[11] N. Li, J. Ren, L. Wang, G. Zhang, P. Hanggi, and B. Li, Phononics: Manipulating heat flow with electronic analogs and beyond, Rev. Mod. Phys. **84**, 1045 (2012).

[12] L. Wang and B. Li, Thermal Logic Gates: Computation with Phonons, Phys. Rev. Lett. **99**, 177208 (2007).

[13] L. Wang and B. Li, Thermal Memory: A Storage of Phononic Information, Phys. Rev. Lett. **101**, 267203 (2008).

[14] P. Ben-Abdallah, Thermal memristor and neuromorphic networks for manipulating heat flow, AIP Adv. **7**, 065002 (2017).

[15] F. Yang, M. P. Gordon, and J. J. Urban, Theoretical framework of the thermal memristor via a solid-state phase change material, J. Appl. Phys. **125**, 025109 (2019).

[16] X. Shen, Y. Li, C. Jiang, and J. Huang, Temperature Trapping: Energy-Free Maintenance of Constant Temperatures as Ambient Temperature Gradients Change, Phys. Rev. Lett. **117**, 055501 (2016).

[17] J. Wang, J. Shang, and J. P. Huang, Negative Energy Consumption of Thermostats at Ambient Temperature: Electricity Generation with Zero Energy Maintenance, Phys. Rev. Applied **11**, 024053 (2019).

[18] J. Ordonez-Miranda, Y. Ezzahri, J. Drevillon, and K. Joulain, Dynamical heat transport amplification in a far-field thermal transistor of vo_2 excited with a laser of modulated intensity, J. Appl. Phys. **119**, 203105 (2016).

[19] K. Ito, K. Nishikawa, A. Miura, H. Toshiyoshi, and H. Iizuka, Dynamic modulation of radiative heat transfer beyond the blackbody limit, Nano Lett. **17**, 4347 (2017).

[20] I. Latella, R. Messina, J. M. Rubi, and P. Ben-Abdallah, Radiative Heat Shuttling, Phys. Rev. Lett. **121**, 023903 (2018).

[21] J. Ren and B. Li, Emergence and control of heat current from strict zero thermal bias, Phys. Rev. E **81**, 021111 (2010).

[22] N. Li, F. Zhan, P. Hänggi, and B. Li, Shuttling heat across one-dimensional homogenous nonlinear lattices with a brownian heat motor, Phys. Rev. E **80**, 011125 (2009).

[23] N. Li, P. Hanggi, and B. Li, Ratcheting heat flux against a thermal bias, Europhys. Lett. **84**, 40009 (2008).

[24] J. Li, Y. Li, P.-C. Cao, M. Qi, X. Zheng, Y.-G. Peng, B. Li, X.-F. Zhu, A. Alù, H. Chen, and C.-W. Qiu, Reciprocity of thermal diffusion in time-modulated systems, Nat. Commun. **13**, 167 (2022).

[25] G. Xu, Y. Li, W. Li, S. Fan, and C.-W. Qiu, Configurable Phase Transitions in a Topological Thermal Material, Phys. Rev. Lett. **127**, 105901 (2021).

[26] J. Ordonez-Miranda, Y. Guo, J. J. Alvarado-Gil, S. Volz, and M. Nomura, Thermal-Wave Diode, Phys. Rev. Applied **16**, L041002 (2021).

[27] A. Salazar, Energy propagation of thermal waves, Eur. J. Phys. **27**, 1349 (2006).

[28] D. Segal, Single Mode Heat Rectifier: Controlling Energy Flow Between Electronic Conductors, Phys. Rev. Lett. **100**, 105901 (2008).

[29] G. Zhang and H. Zhang, Thermal conduction and rectification in few-layer graphene y junctions, Nanoscale **3**, 4604 (2011).

[30] N. Roberts and D. Walker, A review of thermal rectification observations and models in solid materials, Int. J. Therm. Sci. **50**, 648 (2011).

[31] J. Ordonez-Miranda, Y. Ezzahri, J. A. Tiburcio-Moreno, K. Joulain, and J. Drevillon, Radiative Thermal Memristor, Phys. Rev. Lett. **123**, 025901 (2019).

[32] R. Yang, K. L. Chong, Q. Wang, R. Verzicco, O. Shishkina, and D. Lohse, Periodically Modulated Thermal Convection, Phys. Rev. Lett. **125**, 154502 (2020).

[33] P. Urban, P. Hanzelka, T. Králik, V. Musilová, and L. Skrbek, Thermal Waves and Heat Transfer Efficiency Enhancement in Harmonically Modulated Turbulent Thermal Convection, Phys. Rev. Lett. **128**, 134502 (2022).

[34] J. Ordonez-Miranda, Y. Ezzahri, K. Joulain, J. Drevillon, and J. J. Alvarado-Gil, Modeling of the electrical conductivity, thermal conductivity, and specific heat capacity of VO_2, Phys. Rev. B **98**, 075144 (2018).

[35] See Supplemental Material at http://link.aps.org/supplemental/10.1103/PhysRevB.106.L100102 for the details of the propagation of thermal waves in a non-pcm, the maximum heat shuttling, and the temperature evolution of the VO_2 thermal properties.